ISSN 0027-1349, Moscow University Physics Bulletin, 2019, Vol. 74, No. 1, pp. 90–96. © Pleiades Publishing, Ltd., 2019.
Russian Text © B.I. Samolyubov, I.N. Ivanova, 2019, published in Vestnik Moskovskogo Universiteta, Seriya 3: Fizika, Astronomiya, 2019, No. 1, pp. 80–85.

PHYSICS OF EARTH, ATMOSPHERE, AND HYDROSPHERE

Water Dynamics and Diffusion of Admixtures in Lake Onega at Different Stabilities of the Density Stratification

B. I. Samolyubov[1*] and I. N. Ivanova[1]**

[1] *Department of Physics, Moscow State University, Moscow, 119991 Russia*

Received April 5, 2018; revised June 13, 2018; accepted June 15, 2018

Abstract—This article introduces the results of measurements of the distributions of current velocity, temperature, suspended sediments and chlorophyll-a by presence of the drift and density flows, jet and internal waves in Lake Onega. The interpretation of the mechanism of formation of the currents is given. The theoretical distributions of the current velocity and chlorophyll-a are obtained and verified.

Keywords: stratified currents, internal waves, admixture transfer, turbulent exchange, chlorophyll-a.

DOI: 10.3103/S0027134919010144

The processes of the turbulent and wave transfers of admixtures in stratified water-storage basins, lakes, and seas are of particular interest for the development of the methods for the energy and mass exchange forecasting [1–8]. Increased attention in the investigations of such processes is paid to the water dynamics due to the internal waves of various scales [1–5]. A significant part of the studies are devoted to thermocline intrusions, upwelling and downwelling processes, circulations, and vortex structures [4, 6]. Mathematical models analyze and take the effects of hydrophysical processes on the admixture propagation into account by using the data of measurements of the current parameters and water composition. To develop the methods for forecasting the evolution and mass transfer of currents, it is necessary to combine the analysis of the results of in-situ measurements and mathematical modeling. The results of such complex studies are still not sufficiently complete to reveal the mechanisms of the investigated processes and construct models based on these mechanisms. This study is devoted to such investigations. Its aim is to find the regularities in the formation of currents in the presence of internal waves and develop the methods for calculation of the velocity and admixture distributions.

The experimental part of this study was executed during the scientific expeditions of the Department of Physics of Moscow State University in Petrozavodsk Bay of Lake Onega on September 16, 2007 and on July 8–10, 2015. The lake length is 245 km, its width is 88 km, its area is 9943 km^2. The average depth is 30 m, the maximum depth is 120 m. The Coriolis parameter is $1.28\times10^{-4}\mathrm{s}^{-1}$. The average depth of

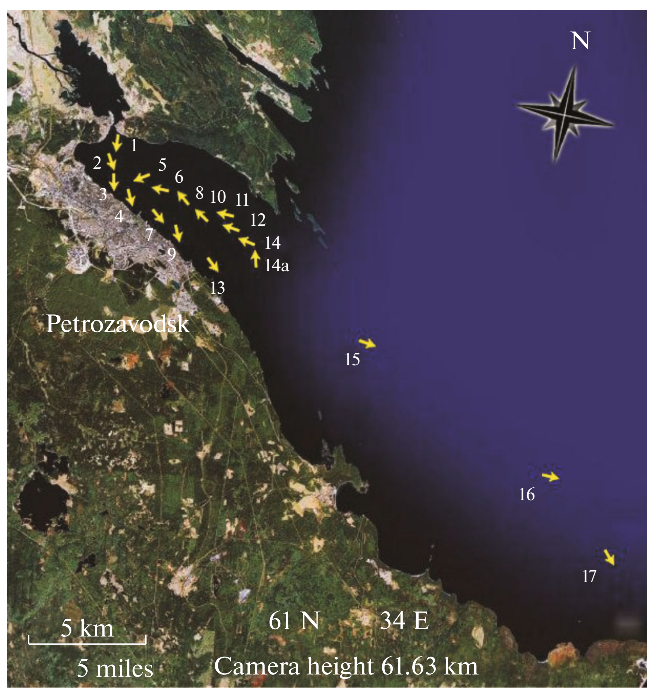

Fig. 1. Map-scheme of vertical aerial photography of the Petrozavodsk Bay with indicated the points of complex sounding on September 16, 2007 and July 08–10, 2015. The photograph of the bay is taken from the data of space photography (Google-Earth).

[*] e-mail: bsamolyubov@gmail.com
[**] e-mail: ivair@yandex.ru

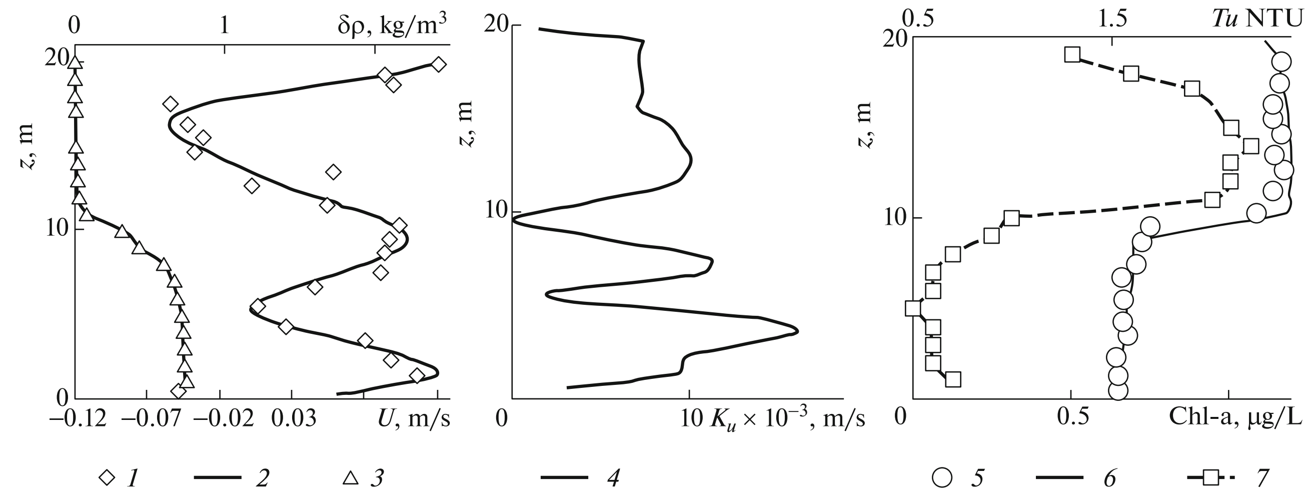

Fig. 2. Profiles of the current velocity U (measured (*1*) and theoretical (*2*), measurements of the water density with the depth (from the surface to the bottom) $\delta\rho$ (*3*), the turbulence exchange coefficient K_u (*4*), chlorophyll-a concentration Chl-a (measured (*5*) and theoretical (*6*), water turbidity (*Tu*)) (in the international nephelometric turbidity units NTU) (*7*) (Petrozavodsk Bay, July 8, 2015).

the Petrozavodsk Bay is 15 m, its maximum depth is 35 m, and its length is 15 000 m [7, 8]. Its main tributary is the Shuya. The structures of the fields of velocity, temperature, suspended sediments and chlorophyll-a concentrations, and conduction at the cross sections along the maximum-depth line and at the stations (Fig. 1) were studied. The measurements were carried out from the "Ekolog" research station of the Northern Water Problems Institute of the Karelian Research Center of the Russian Academy of Sciences with the RCM9LW (Aanderaa Instruments) and CTD90M (Sea-Sun) sounders with a Doppler velocity sensor, sensors of temperature, conduction, water turbidity, and oxygen and chlorophyll-a concentrations. The meteorological parameters were measured simultaneously. The object, investigation methods, and the used instruments were described in detail in [6]. The analysis of the results and theoretical studies were based on the new approaches and methods developed earlier [2–9].

1. THE STRUCTURE OF THE CURRENT, TEMPERATURE, AND ADMIXTURE CONCENTRATION FIELDS

In this section, we consider the results of the expedition that took place in 2015 for the first time. Unlike the data of 2007 [9] which were obtained under the conditions of the transition to the autumnal homothermy in the lake at $(Ri_H)_a$=15, $(\overline{\Delta\rho_H})_a = 0.3$ kg/m^3 and $(\overline{U_H})_a$=0.04 m/s, the data of 2015 were obtained during a period of stable stratification at $(Ri_H)_a$=70, $(\overline{\Delta\rho_H})_a = 0.7$ kg/m^3 and $(\overline{U_H})_a$= 0.07 m/s. Here, $Ri_H = g\overline{\Delta\rho_H}H/\rho\overline{U}_H^2$ is the integral (with respect to the depth) Richardson number, g is the free fall acceleration, $\Delta\rho_H$, H, $\overline{U}_H$ are the difference between the water densities near the bottom and the surface, the depth of the place, and the depth-averaged velocity, respectively; a is the section-averaging index. The number Ri_H is applied when modeling the wind-wave currents as a characteristic of the total hydrodynamic stability [10]. The velocity of the wind directed towards the open lake varied from 6 to 8 m/s.

The structure of the velocity field at the cross section along the maximum-depth line of the bay was determined by the drift current, the jet in the thermocline, near-bottom flow, and other currents caused by the internal seiches (Fig. 2). These profiles are measured at the second from nine verticals of the cross section at a distance of 2 km from its beginning in the bay headwaters.

The maximum jet velocity at the profile is 0.05–0.2 m/s at depths of 6–20 m. The total depth at the cross section is 16–29 m. The jet thickness is 9–17 m, the average Richardson number at the cross section in it $Ri_j = g\Delta\rho_j\Delta z_j/\rho U_{mj}^2$ is 2. Here, $\Delta\rho_j$, Δz_j, U_{m_j} are the difference between the water densities in the jet and above it, the thickness, and the maximum of jet velocity, respectively.

The near-bottom flow velocity is up to 0.06 m/s, its average thickness is 6 m, and the average Richardson number at the cross section $Ri_u = g\overline{\Delta\rho}z_u/\rho\overline{U}^2$ is approximately 8. Here, $\overline{\Delta\rho}$, Δz_u, and $\overline{U}$ are the difference between the water densities in the flow and above it, the thickness, and the average current velocity, respectively.

The peak U with a value from -0.15 to 0.15 m/s at a depth of 5 ± 3 m is determined by the second mode of the internal wave in the active layer. Usually, the second mode has the most significant influence on the jet in the thermocline region. The wavelength for this mode is 4000 m; its period is approximately 6 h. In other layers, the wave component is not as well pronounced at the profile $U(z)$.

The curve $U(z)$ in Fig. 2 is plotted by using a modified algorithm that combines the approaches developed in [6, 11] for the internal waves and in [6, 7, 8] for the near-bottom drift flows and the jet. The composition of the profiles of the velocity of these currents, internal waves with periods of 23 ± 4, 11.4 ± 1 h, and the principal mode of the second wave (5.7 ± 0.5 h) is applied. The theoretical profiles agree with those measured (Fig. 1). The main periods in the spectrum of the internal waves of Lake Onega are 12, 6, 24, and 63 h [3]. When calculating the velocity profiles at the cross section, we used wave periods close (with a spread of approximately 1 h) to the first and second periods from the spectrum [3]. The vertical wavelengths are determined by the depths of the place of measurements and the thermocline. The internal waves' phase velocity c_w was 0.15–0.21 m/s; the waves' heights $h_w = 1 - 5$ m. Here, $c_w = (g\Delta\rho_T h_T(H - h_T)/\rho H)^{1/2}$, according to [11], h_T is the thermocline depth, H is the basin depth, $\Delta\rho_T$ is the difference between the water densities in the layers h_T and $H - h_T$. The water density ρ was determined from the measured parameters of the water state according to the Chen–Millero equation [12].

The depth of the internal wave induced by wind was determined from the formula $h_w = 3.2 \times 10^{-6} k_L \rho U_w^2 L_G / gH\Delta\rho_T$, where U_w is the wind velocity, L_G is the bay length. Here, k_L is the coefficient that allows for the stability range of stratification, the thermocline depth, the lake topography, effective values of the wind action time, and the fetch for the near-surface seiche that generates the internal seiche, and other factors [13]. In the cases we considered at two cross sections, the average value of k_L was 0.2.

The profile of the turbulent exchange coefficient $K_u = (u_\tau + u_c)\ell/(1 + \alpha_2 Ri_d)^{1/2}$(according to [8]) contains peaks in the mixing layers of the density, jet, wave, and drift currents (Fig. 2, curve *4*). Here, $Ri_d = N^2\ell^2/(u_\tau + u_c)^2$ is the modified Richardson number, $N = (g(-\partial_z\rho)/\rho)^{1/2}$ is the buoyancy frequency, $u_\tau = \ell|\partial_z U|$ is the shift velocity, ℓ is the turbulence scale [11], $u_c = 0.02\overline{U_{FD}}\left(1 - |\partial_z U|/|\partial_z U|_{\mathrm{MAX}}\right)$, $\overline{U_{FD}}$ is the depth-average modulus of velocity. At the average $\overline{K_u} = 7.6 \times 10^{-3}$ m^2/s, the maximum values of K_u at the profile are 2, 1.5, and $1.3\overline{K_u}$. The zones of the maximum values of K_u in the upper layer of jet mixing, in the wave and drift currents at $z > 10$ m overlap.

At the profile of the water turbidity Tu, in addition to its increase with the depth in the near-bottom layer, there is a maximum above the thermocline in the jet mixing layer (Fig. 2, curve *5*). The maximum of the exchange coefficient K_u is located in the same region. In this region, the suspension sedimentation from the near-surface layers decelerates; thus, Tu increases.

Such a peculiarity is absent at the profile of the chlorophyll-a (Chl-a) concentration (Fig. 2, curves *5*, *6*) because of a high intensity of mixing and an insignificant cosedimentation of phytoplankton and suspension particles. Curve *6* is theoretical; it is calculated according to model for the Chl-a transfer that we proposed. The part of the model related to calculations of the current velocity, turbulent exchange coefficient, and other hydrophysical parameters and the algorithm of solving were developed earlier [8]. Special characteristics of the Chl-a transfer are considered in the model as in [18]. The model also contains the Chl-a transfer rate that depends on temperature, with a residual flow associated with the unaccounted processes (hydrochemical, hydrobiological, etc.). The expressions are applied that were found for determining the boundary conditions: a) for the Chl-a concentration at a height of 1 m from the bottom and at a depth of 0.5 m from the surface, b) for the vertical turbulent Chl-a flow at a depth of 0.5 m. The standard deviation from the theoretical profiles at the cross section did not exceed 15%.

In the water temperature field T (Fig. 3a) we distinguished a cold near-bottom layer in the density current region with wave oscillations of isotherms at its upper boundary. Above, there is a region of warmer waters in the upper layer of jet mixing. Despite the local rise in temperature (on average over the cross section by 0.1°C), the jet keeps its stability. The decreases in T near the surface occur under the conditions of the increase in the wind velocity within an interval from 6 to 8 m/s.

In the turbidity field (Fig. 3b) at the cross section beginning, we observed the appearance of a near-surface and a near-bottom nepheloid layers that are characteristic for the levee zones. The further transformation of this structure at the cross section is due to sedimentation and the influence of currents and internal waves.

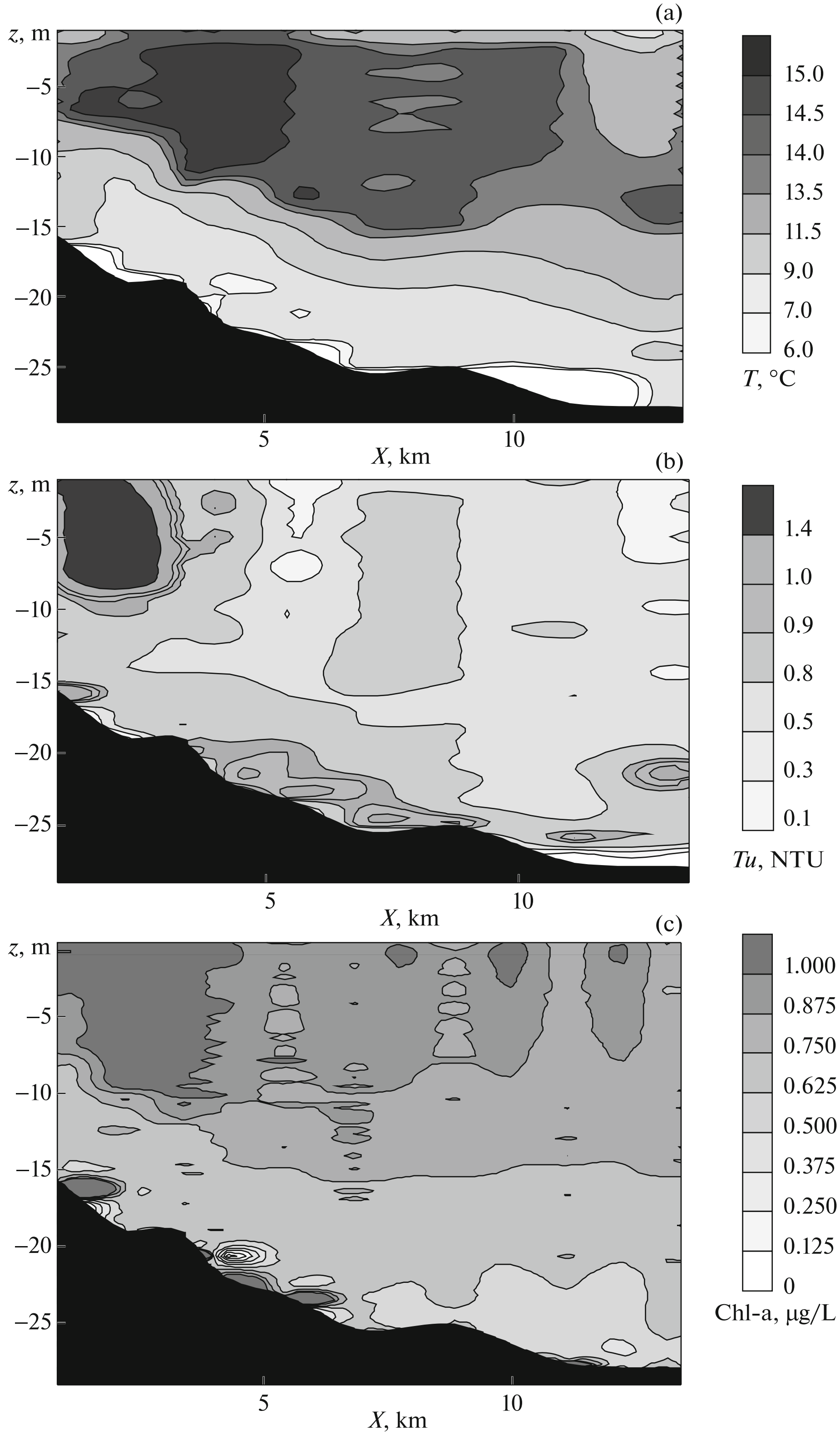

Fig. 3. Distributions of (a) temperature T, (b) turbidity Tu, and (c) chlorophyll-a concentration over the depth and along the cross section (Petrozavodsk Bay, July 8, 2015).

In the Chl-a concentration field (Fig. 2, curve *5*); Fig. 3c) a decrease occurs in the depth down to one-tenth when passing from the epilimnion to the hypolimnion and to one-half along the cross section.

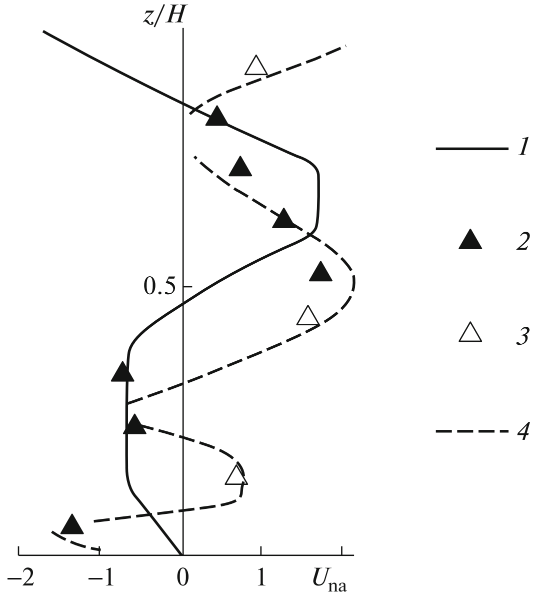

Fig. 4. Profiles of current velocity U_{na}: (*1*) theoretical from [13] (without consideration of the drift and density flows) and (*2*), (*3*) measured according to the results of our study (Petrozavodsk bay, July 8, 2015, the third vertical line of the cross section from the upper bay to the open lake). Here, *3* is the designation of the profile's points whose deviations from the curve under the influence of other currents violate the general qualitative agreement with curve *1*; *4* is the theoretical profile of the velocity from this study (with consideration of the drift and density flows and upwelling), H is the total depth of the place, U_{na} is the velocity normalized to its modulus-average value at this vertical line.

The outbursts of concentration near the bottom and in the beginning of the cross section occur due to the currents of wave origin.

2. ON THE MECHANISMS OF THE FORMATION OF THE NEAR-BOTTOM FLOW AND JET

The estimates of the water flow rate in the tributary to the Petrozavodsk Bay from the Shuya show that the inflow of these waters cannot provide the jet and near-bottom flow in the bay.

Another source of the inflow of cold near-bottom waters to the bay is upwelling from an open lake under the action of large-scale internal waves with periods of 63 h and larger (Section 1) at a duration of performing the longitudinal-axial cross section of the Petrozavodsk Bay of 12.5 h. The upwelling is followed by the downwelling that is enforced by a cold gravitational stratified flow descending along the slope (the density flow). Depending on the density flow velocity, it can not only intensify the downwelling but exceed the upwelling and, thus, decelerate it at

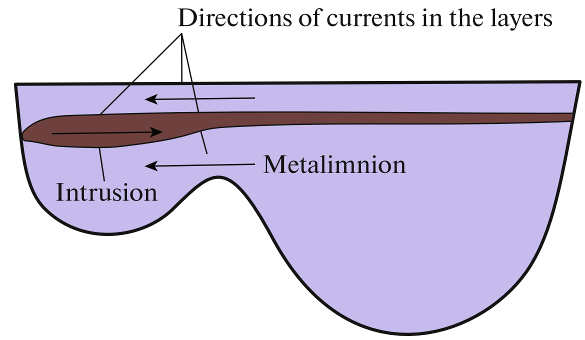

Fig. 5. Scheme of the intrusion of the jet generated by the reflected internal wave [5].

the beginning stages of its development. The section-average ratio of the theoretical maximum velocity of the gravity flow estimated in the SGO-current U_{SGO} approximation to the maximum measured velocity of the near-bottom current at the profile U_m is 1.5. This confirms the assumption about a leading role of the gravity flow for the development of the near-bottom current, whose generation is related to the influence of the large-scale internal waves on the water dynamics. Here, $U_{SGO} = \left(gz_u i_s \overline{\Delta\rho}/\rho C_D\right)^{1/2}$, z_u is the density flow thickness, i_s is the bottom slope, C_D is the drag coefficient at the flow—bottom boundary whose section-average value is 5×10^{-3}.

The jet formation in the thermocline region is highly likely to be related to the influence of the large-scale internal wave reflected at the shallow water due to which the jet flow occurs in the direction towards the open lake [5]. This process is illustrated by the velocity profile in Fig. 4 in the intrusion scheme in Fig. 5. The gravitational acceleration leads to the jet intensification because of the sloping of the isopycnic surfaces with growing depth. According to Fig. 4, the measured distribution $U(z)$ *2*, *3* qualitatively agrees with the theoretical distribution *1* from [5] that is plotted with no consideration of the drift, density flows, and the wave upwelling. Here, *3* are the points at the profile whose deviations from curve *1* under the influence of the mentioned currents violate the general accordance, including the deviation at the height $z/H = 0.2$, which is associated with the influence of the gravitational flow. These flows are taken into account in the composition distribution *4* plotted by using the algorithm of this study. The composition *4* also includes the wave upwelling flow above which the density flow increases slightly.

The presented analysis proves the wave mechanisms of the jet and near-bottom current formation. The generation of these currents is due to the influence of their stratification, gravitational components, and internal waves with wavelengths of the order of the entire like scale on the water dynamics. The

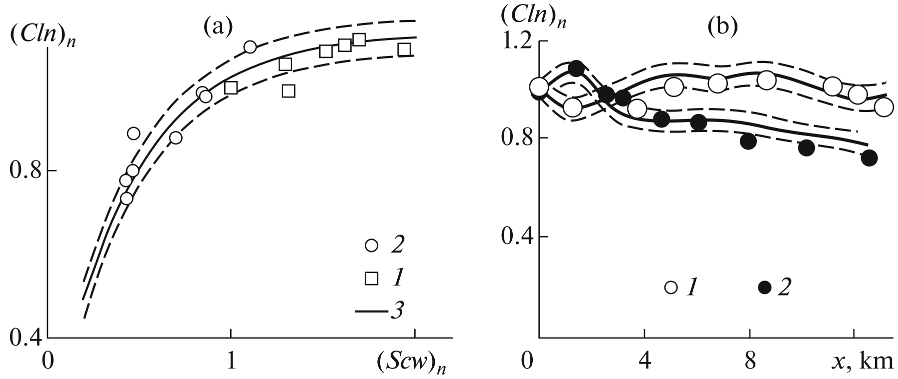

Fig. 6. Dependence of the chlorophyll-a concentration averaged over the active layer's depth and normalized to the initial value (at $x = 0$), $(Chl)_n$ (a) on the normalized in the same way wave flow of suspension $(Scw)_n$ and (b) on the distance x along the cross section. Designations *1*, *2* in Figs. 6a, 6b relate to the data obtained at the cross sections on September 16, 2007 and July 8–10, 2015, respectively. The curve in Fig. 6a is the approximation by the saturation function; the curves in Fig. 6b are those derived from the diffusion equation. the dotted lines are the boundaries of the standard deviation.

period of such waves $t_{w\ell s} = 63$ h (Section 2 of this paper) is five times higher than the measurement duration at the longitudinal-axial cross section of the bay t_{cross}. Thus, in the interval $t_{\text{cross}} = 0.2t_{w\ell s}$, the wave phase may remain sufficiently close to that which is necessary for jet formation, the more so as the period t_{wk} is presented in [3] as the minimum for such internal waves.

3. THE CHLOROPHYLL-a DISTRIBUTION ALONG THE CROSS SECTION

According to the results of [14–17], the influence of currents and internal waves leads to an increase in the biological productivity due to the nutrient transfer to the photic layer. It is noted that mathematical models for the phytoplankton distribution must consider the wave transfer because of the powerful influence of the internal waves on the active layer illumination and, correspondingly, on the phytoplankton development [16].

It is shown that in the dissipation zones, where the surface and deep water mixing is more efficient, the intensification of the biological productivity by currents and internal waves is especially noticeable [16]. Complex investigations have allowed us to establish that the internal waves intensify photosynthesis, since they transfer phytoplankton in the nonlinear light field [17]. A significant role is played by the wave-induced changes in the water composition, which are important for phytoplankton production.

According to the data we obtained, the Chl-a concentration in the active layer is proportional to the wave height in the first half of the day. The effect of its growth is related to the photosynthesis intensification during the wave upwelling. The discovered dependence of the Chl-a concentration on the wave flow of suspended sediments Sc_w that has the form $(Chl)_n \cong k_{cs} - \exp\left(-2k_{cs}\left(Sc_w\right)_n\right)$, where $k_{cs} = 1.13$ (Fig. 6a) is important to predict the Chl-a distribution. This dependence attains saturation with growing S, which is due to the fact that the illumination is reduced because of the influence of suspension.

Particular interest is raised by the joint effect of the intrathermocline stratified jet and internal wave on the Chl-a concentration. It follows from the analyzed data that the Chl-a concentration negatively correlates with the water discharge per unit of flow width $q_j = \overline{U}_j \Delta z_j$, where $\overline{U}_j$ and Δz_j are the vertical-average velocity and jet thickness, respectively. However, this correlation is not high enough to satisfy the conservative condition for the admixture.

The longitudinal distribution of the chlorophyll-a concentration averaged over the jet thickness $\overline{Chl}_j(x)$ was found from the following system of the diffusion and continuity equations:

$$\partial_t Chl + U\partial_x Chl + (W - \omega_{fc} + \omega_{RT})\partial_z Chl = -\partial_z \langle W'Chl' \rangle, \tag{1}$$

$$\partial_x U + \partial_z W = 0. \tag{2}$$

In (1) and (2), U and W are the longitudinal and vertical components of the average current velocity, respectively; Chl' are the pulsations of the Chl concentration; W' are the pulsations of the velocity W. Equation (1) also contains the rates of phytoplankton sedimentation ω_{fc} and the total quantity ω_{RT}, which corresponds to the Chl flows due to illumination, provision with nutrients, and other factors [15]. The velocities ω_{fc} and ω_{RT} were taken to be zero. We used the passive admixture approximation (the Schmidt number Sc in the expression for the turbulent flow $\langle W'Chl' \rangle$ [8] was taken to be 1).

When calculating W, the changes in the jet thickness and its trajectory (including wave changes) were considered. This made it possible to take the influence of the internal waves on the jet and the chlorophyll-a transfer in it into account.

Equation (1) was integrated over the vertical line (the jet thickness) by using an algorithm analogous to that presented in [8] with consideration of the peculiarities of the jet current and chlorophyll-a transfer. In the quasi-stationarity, two-dimensionality, and other approximations presented in [7, 8], with the substitution of W according to (2), equation (1) is transformed to the form that has a solution for the distribution $\overline{Chl}_j\,(x)$ in quadratures. Using this solution, at the given velocity and water density distributions and the initial admixture concentration (at $x = 0$), the values of $\overline{Chl}_j\,(x)$ can be found.

On the whole, the theoretical distributions agree with those measured (Fig. 6b). The discrepancy between the obtained distributions at two cross sections can be explained mainly by the increase in the influence of the stability (Section 1), which results in the decrease in the concentration with a distance along the jet at the cross section of 2015. As for the estimation of the role of the internal waves among other hydrodynamical processes in the Chl-a transfer [14–17], taking the interpretation of the mechanisms of formation of the currents, presented in Section 2 into account we can consider that this role is the most significant for the processes we have dealt with in this study.

CONCLUSIONS

In conclusion, it should first of all be noted that the influence of the internal seiches on the water dynamics leads to formation of the revealed system of stratified currents that includes, in addition to the drift current, a near-bottom flow and an intermediate jet in the thermocline region. The proposed procedure of theoretical description of the velocity profiles agrees with the data obtained for different hydrodynamical conditions. The found dependence of the chlorophyll-a distribution on the wave suspension flow that has an ascending character and attains saturation is important for forecasting the chlorophyll-a distribution. In addition to the methods developed earlier, the key role in the calculations of the chlorophyll-a concentration distribution was played by the following factors:

(1) the expressions found for determining the boundary conditions when obtaining the vertical profile;

(2) the consideration of the changes in the jet thickness and its trajectory when obtaining the longitudinal concentration distribution in the jet.

ACKNOWLEDGMENTS

This work was supported by the Russian Foundation for Basic Research, project no. 14-05-00822.

REFERENCES

1. J. VidaI, S. MacIntyre, E. E. McPhee-Shaw, et al., Limnol. Oceanogr. **58**, 1557 (2013). https://doi.org/10.4319/lo.2013.58.5.1557
2. A. Gomes-Giraldo, J. Imberger, J. P. Antenucci, and P. S. Yates, Limnol. Oceanogr. **53**, 354 (2008).
3. N. Filatov, A. Terzevik, R. Zdorovennov, V. Vlasenko, N. Stashchuk, and K. Hutter, in *Nonlinear Internal Waves in Lakes*, Ed. by K. Hutter (Springer, 2012), p. 23.
4. L. Umlauf and U. Lemmin, Limnol. Oceanogr. **50**, 1601 (2005).
5. J. Appt, J. Imberger, and H. Kobus, Limnol. Oceanogr. **49**, 919 (2004).
6. B. I. Samolyubov and I. N. Ivanova, Phys. Wave Phenom. **23**, 76 (2015). https://doi.org/10.3103/S1541308X15010124
7. B. I. Samolyubov, *Density Currents and Impurity Diffusion* (URSS, Moscow, 2007).
8. B. I. Samolyubov, Moscow Univ. Phys. Bull. **67**, 398 (2012). https://doi.org/10.3103/S0027134912040121
9. K. V. Pokazeev, B. I. Samolyubov, and N. N. Filatov, Russ. Meteorol. Hydrol. **37**, 130 (2012).
10. K. Michioku, J. Hydrosci. Hydraul. Eng., No. SI-1, 17 (1993).
11. L. Prandtl, *Führer durch die Strömungslehre* (F. Vieweg, 1942).
12. C. Chen and F. Millero, Limnol. Oceanogr. **31**, 657 (1986).
13. R. A. Bryson and R. A. Ragotzkie, Limnol. Oceanogr. **5**, 397 (1960). https://doi.org/10.4319/lo.1960.5.4.0397
14. J. C. Sanchez-Garrido, C. Naranjo, D. Macias, et al., J. Geophys. Res.: Oceans **120**, 7329 (2015). https://doi.org/10.1002/2015JC010885
15. Y. Cuypers, B. Vincon-Leite, and A. Groleau, ISME J. **5**, 580 (2011).
16. X. Pan, G. T. F. Wong, F. Shiah, and T. Ho, J. Oceanogr. **68**, 427 (2012). https://doi.org/10.1007/s10872-012-0107-y
17. M. A. Evans, S. MacIntyre, and G. W. Kling, Limnol. Oceanogr. **53**, 339 (2008).
18. G. P. Astrakhantsev, V. V. Menshutkin, N. A. Petrova, and L. A. Rukhovets, *Simulation of Ecosystems of Large Stratified Lakes* (Nauka, St. Petersburg, 2003).

Translated by E. Smirnova